Author/s:
Steward, CE;Venkatraman, VK;Lui, E;Malpas, CB;Ellis, KA;Cyarto, EV;Vivash, L;O'Brien, TJ;Velakoulis, D;Ames, D;Masters, CL;Lautenschlager, NT;Bammer, R;Desmond, PM

Title:
Assessment of the DTI-ALPS Parameter Along the Perivascular Space in Older Adults at Risk of Dementia

Date:
2021-05-01

Citation:
Steward, C. E., Venkatraman, V. K., Lui, E., Malpas, C. B., Ellis, K. A., Cyarto, E. V., Vivash, L., O'Brien, T. J., Velakoulis, D., Ames, D., Masters, C. L., Lautenschlager, N. T., Bammer, R. & Desmond, P. M. (2021). Assessment of the DTI-ALPS Parameter Along the Perivascular Space in Older Adults at Risk of Dementia. Journal of Neuroimaging, 31 (3), pp.569-578. https://doi.org/10.1111/jon.12837.

Assessment of the DTI-ALPS parameter along the perivascular space in older adults at risk of dementia

Christopher E. Steward [1#], Vijay K. Venkatraman [1#], Elaine Lui [1], Charles B. Malpas [1,2], Kathryn A. Ellis [4,7], Elizabeth V. Cyarto [6], Lucy Vivash[1,2,8], Terence J. O'Brien [1,8], Dennis Velakoulis [11], David Ames [4,9,10], Colin L. Masters [3], Nicola T. Lautenschlager [4.5*], Roland Bammer [1*], and Patricia M. Desmond [1*]

[1]Department of Medicine and Radiology, University of Melbourne, Melbourne, Australia, [2]Department of Neurology, Royal Melbourne Hospital, Melbourne, Australia, [3]Florey Institute for Neuroscience and Mental Health, [4] Academic Unit for Psychiatry of Old Age, Department of Psychiatry, The University of Melbourne, Melbourne, Australia, [5] NorthWestern Mental Health, Melbourne Health, Melbourne, Australia, [6] Bolton Clarke Research Institute, Brisbane, QLD, Australia,[7] Melbourne School of Psychological Sciences, The University of Melbourne, Melbourne, Australia, [8] Department of Neurosciences, Central Clinical School, Monash University, Melbourne, Australia, [9] National Ageing and Research Institute, Melbourne, VIC, Australia, [10] St George's Hospital, Kew, VIC, Australia, [13] Neuropsychiatry Unit, Royal Melbourne Hospital &

Melbourne Neuropsychiatry Centre, University of Melbourne, Melbourne, VIC, Australia.

Joint first authors, * Joint senior authors

Acknowledgments and Disclosures

We are most grateful to all volunteers taking part in the study and to the research and clinical staff from following institutes in Melbourne, VIC, Australia: the Department of Psychiatry, The University of Melbourne, the National Ageing Research Institute (NARI), the Mental Health Research Institute (MHRI) and the Department of Medicine and Radiology at the Royal Melbourne Hospital.

The authors declare that this study received funding from Australia's National Health and Medical Research Council; Contract grant number: 1005492. Funding for the AIBL study is provided by the CSIRO Flagship Collaboration Fund and the Science and Industry Endowment Fund (SIEF) in partnership with Edith Cowan University (ECU), Mental Health Research institute (MHRI), Alzheimer's Australia (AA), National Ageing Research Institute (NARI), Austin Health, CogState Ltd., Hollywood Private Hospital, Sir Charles Gardner Hospital. The study also received funding from the National Health and Medical Research Council, the Dementia Collaborative Research Centres program

(DCRC2) and The McCusker Alzheimer's Research Foundation and Operational Infrastructure Support from the Government of Victoria. The funder was not involved in the study design, collection, analysis, interpretation of data, the writing of this article or the decision to submit it for publication. The imaging data and cognitive data collection for the Alzheimer's cohort was funded by Velacor Therapeutics as part of the VELACOR-002 trial.

Background and Purpose: Recently, there has been growing interest in the glymphatic system (the functional waste clearance pathway for the CNS) and its role in flushing solutes (such amyloid ß and tau), metabolic and other cellular waste products in the brain. Herein, we investigate a recent potential biomarker for glymphatic activity [the Diffusion Tensor Imaging Along the Perivascular Space (DTI-ALPS) parameter] using Diffusion MRI imaging in an elderly cohort comprising 10 cognitively normal, 10 Mild Cognitive Impairment (MCI), and 16 Alzheimer's disease (AD) .

Methods: All 36 participants imaged on a Siemens 3.0T Tim Trio. Single-SE diffusion weighted Echo-planar imaging scans were acquired as well as T1 Magnetization Prepared Rapid Gradient Echo, T2 Axial and Susceptibility

Weighted Imaging. 3mm regions of interest were drawn in the projection and associations fibres adjacent to the medullary veins at the level of the lateral ventricle. The DTI-ALPS parameter was calculated in these regions and correlated with cognitive status, Mini-Mental State Examination (MMSE) and ADASCog11 measures.

Results: Significant correlations were found between DTI-ALPS and MMSE and ADASCog11 in the right hemisphere adjusting for age, sex and APoE ε4 status. Significant differences were also found in the right DTI-ALPS indices between cognitively normal and AD groups ($p < 0.026$) and MCI groups ($p < 0.025$) in a univariate General Linear Model corrected for age, sex and APoE ε4. Significant differences in Apparent Diffusion Coefficient between cognitively normal and AD groups were found in the right projection fibres ($p=0.028$)

Conclusion: Further work is needed to determine the utility of DTI-ALPS index in larger elderly cohorts and whether it measures glymphatic activity.

Introduction

There is currently significant interest in the glymphatic system[1-3] – the functional waste clearance pathway for the CNS – and its role in removing solutes (such as amyloid-β and tau), metabolic, and other cellular waste products from the brain. So much so, that the term "Neurofluids"[4] has been coined lately to describe collectively the various fluids (venous, arterial, cerebrospinal fluid (CSF), and interstitial fluid (ISF)) present in the extracellular brain compartments, and is a useful term when discussing the glymphatic system. It is hoped that a knowledge of neurofluid dynamics, and how "open" these fluid channels are in the presence of neurological conditions, will greatly assist in our understanding of glymphatic system related diseases. For example, it has been hypothesized that a failure in the clearance of soluble amyloid-β from the brain's interstitial space contributes to accumulation of amyloid plaques and Alzheimer's Disease (AD) progression.[5,6] Glymphatic function may therefore be used as a potential biomarker of AD progression. Measurements of glymphatic dynamics have mainly been performed in animal MRI studies. Adoption in human studies has been limited, due to the need for

intrathecal administered tracers[7] with serial imaging to track fluid movement over longer periods of time.

However, a range of new techniques is being investigated to help assess glymphatic function.[8-12] One recent study[13] applied Magnetic Resonance (MR) Diffusion Tensor Imaging (DTI) for this purpose. The study identified projection and association fibres orthogonal to the perivascular space at the level of the lateral ventricles, and developed an index referred to as Diffusion Tensor Imaging Along the Perivascular Space (DTI-ALPS) that measured water diffusion aside the perivascular space which if verified might be used as a proxy marker for glymphatic function. That study showed significant positive correlations between DTI-ALPS and cognitive function assessed with the Mini-Mental State Examination (MMSE),[14] as well as significant negative correlations between the mean diffusivities of the projection fibres (adjacent to the lateral ventricle) and association fibres (superior longitudinal fascicles) with MMSE scores.

Other studies[15,16] have also made use of the DTI-ALPS index in both patients with Parkinson's Disease and Idiopathic Normal Pressure Hydrocephalus. DTI-ALPS showed promising results in its ability to differentiate between these disease groups, but currently there is a paucity of evidence for its utility in people with or at risk of dementia. Therefore, in this study, we aimed to

evaluate DTI-ALPS in 26 people with either mild cognitive impairment (MCI) or established AD and 10 cognitively normal participants (controls). We also investigated whether there are any relationships between the DTI-ALPS index and cognitive groups, as well as with two measures of cognitive function, MMSE and ADAS-Cog11.[17]

Methods

Participants

The sample in this study was drawn from data of two clinical trials. The first trial cohort consisted of 108 older volunteers with subjective memory complaints or mild cognitive impairment, living in the Melbourne metropolitan area (median age [IQR] - 73 years [67.25,76.0]), recruited from participants of the Australian Imaging, Biomarkers and Lifestyle (AIBL Active) study[18] of whom MR scans from 20 of these were selected for inclusion in this study. The 16 participants living with AD were recruited from the VEL015 trial[18] which was a randomized double-blind controlled trial of sodium selenate in people with mild-moderate AD to assess tolerability, and efficacy in varying selenium concentration in the central nervous system (CNS). Identical imaging protocols were used for both trials and on the same scanner. All scans were acquired on

the same MR scanner. The inclusion and exclusion criteria and power calculation for the AIBL Active RCT have been published in the trial protocol paper,[19] and for the VEL015 trial here.[20] The sample data was derived from the original data in both trials to ensure there was no selection bias in age, sex, or APoE ε4. Demographic information for the samples in this study is given in Tables 1 and 2. There were no significant differences in age, sex or APOE ε4 between the drawn samples and the population.

MR Imaging

All 36 participants underwent MR imaging, after providing written consent, following recruitment on a Siemens 3.0T Tim Trio (Siemens Healthineers, Erlangen, Germany) using the system's 12-channel head array coil at the Royal Melbourne Hospital as part of the AIBL Active study[19] and VEL015 study.[20,21] The MR sequences were as follows:

1. Single-SE diffusion-weighted Echo-planar imaging (EPI) were acquired: Repetition Time (TR)/Echo Time (TE) = 8700/92 ms, Field-of-view (FOV) 240 x 240 mm, matrix 96 x 96, b = 1000 s/mm^2, voxel size 2.5 mm^3, 30 directions (gradient direction definitions as provided by vendor);
2. Susceptibility weighted Imaging using 3D gradient recalled echo and Minimum Intensity Projection (mIP) images: TR/TE=40ms/30ms, FOV =

164x250mm , matrix=336x512, voxel size 0.48x0.48x4mm, α=15°); 3. Structural T_1-weighted Magnetization Prepared Rapid Gradient Echo: TR/TE/Inversion Time=1,900/2.13/900ms, FOV=256×256mm, matrix=256×256, α=9°, voxel size 1 mm^3, bandwidth/pixel 219 hz; and 4. 2D T2-weighted TSE axial images: TR/TE= 3000/98 ms; FOV=256×256mm, matrix, 512x512, voxel size 0.5x0.5x3mm, bandwidth/pixel 130 Hz, and turbofactor 21.

Diffusion Image Analysis

In this study, we were interested in measuring proton diffusion metrics along the perivascular space in regions of interest drawn by a neuroradiologist in order to calculate the DTI-ALPS index. To do this, required accurate identification of medullary veins structures at the level (slice) of the lateral ventricles. The perivascular spaces run concentrically along these veins. These fine veins cannot be seen on diffusion images and can be best identified on Susceptibility-Weighted Imaging (SWI) scans. In order to precisely overlay both Diffusion-Weighted Imaging (DWI) and SWI scans to measure diffusion values in the correct regions, for each patient the DWI and SWI scans were both co-registered to a common space of the high-resolution T2-axial scans.

The diffusion-weighted MRI data were initially pre-processed using the Tortoise software package (National Institutes of Health, Bethesda, Maryland, v3.1.1).[22,23] The raw DWI were Anterior Commissure (AC)-Posterior Commissure (PC) corrected and the skull removed using AFNI.[24] Moreover, Tortoise corrected the data for Gibbs ringing artefacts, subject motion and eddy-current artefacts, as well as EPI susceptibility distortions using DIFFPREP.[22,23] The T2-weighted axial scans were also AC-PC corrected using standard AFNI scripts to register the T1-weighted structural images to MNI152 space, and the T2-weighted images to the T1. Diffusion tensors were then calculated (informed RESTORE) on a per pixel basis and registered to the AC-PC-corrected T2-weighted images using ANTS.[25] The minimum intensity projection (mIP) images were visually better suited than the SWI for co-registration to the T2-weighted images, and the elastic transformations derived from this applied to the SWI images to transfer them to T2-space. The co-registered SWI and DTI images were visually checked to ensure anatomical agreement.

With FSLEyes[26] the V1 (primary eigenvector)-color-indexed fractional diffusion anisotropy maps (which were derived from the aforementioned DTI scans) and SWI images were overlayed and a qualified neuro-radiologist with over 25 years of experience marked two 3mm spherical regions of interest

(ROIs) in the region of the projection and association fibres for both hemispheres and adjacent to the medullary veins at the level of the lateral ventricle (Figure 1). Care was taken to ensure that the ROI's lay exclusively in the selected fibre tracts. The DTI-ALPS index[13] measures the ratio of the mean of the *x*-axis diffusivity in the area of projection fibres ($D_{x,proj}$) and *x*-axis diffusivity in the area of association fibres ($D_{x,assoc}$) to the mean of *y*-axis diffusivity in the area of projection fibres ($D_{y,proj}$) and *z*-axis diffusivity in the area of association fibres ($D_{z,assoc}$) and is given by:

$$\text{ALPS index} = \text{mean}(D_{x,proj}, D_{x,assoc})/\text{mean}(D_{y,proj}, D_{z,assoc}).$$

It has been used as a proxy for glymphatic activity[13] and was calculated for each participant in this study. Thereafter, its relationship was assessed with the individual MMSE and Alzheimer's Disease Assessment Scale–Cognitive Subscale (ADAS-Cog11) scores. DTI-ALPS values near 1 indicate little diffusion along the perivascular space, whilst higher values include greater diffusivity. All co-registrations herein were visually inspected. A diagram of the main aspects of the processing pipeline is given in Figure 1.

Cognition Scores and APoE ε4

The MMSE cognitive performance scores were obtained for all participants.[14,27] Moreover, the Memory Complaint Questionnaire (MAC-Q) score[28] was used to determine perceived cognitive decline in the 10 cognitively normal participants. The Consortium to Establish a Registry for Alzheimer's Disease (CERAD*)* neuropsychological assessment battery was employed to identify 10 participants with MCI from the AIBL cohort.[29] The 16 participants living with AD were diagnosed with probable AD according to NINCDS-ADRDA criteria.[30] Presence of at least one APoE ε4 allele was determined from baseline blood samples.

Statistical Methods

All statistical analyses, including demographics, partial correlations, and general linear models were performed with SPSS 26.0.[31] Independent sample t-tests were used to compare DTI-ALPS index between cognitive groups and Cohen's d to calculate effect-sizes (Tables 3 and 4). Partial correlations (in Table 5) used two-tailed testing. A univariate general linear model was used (in Table 6) to examine the association of DTI-ALPS index between all three

cognitive groups, adjusted for age, and two dichotomous variables, sex and APoE ε4.

Results

In Table 1, the demographics (age, sex) and cognitive information for each participant are given. Summary statistics in Table 2.

In Figure 2a and 2b, the location of the 3mm spherical ROIs used to assess the DTI-ALPS index for each participant are displayed. The normally overlaid SWI and V1 maps have been separated here for viewing purposes. Projection fibres are labelled blue, and association fibres green.

In Tables 3 and 4, the results for the DTI-ALPS index measures are given, with mean values for each cognitive group listed in Table 3, and effect-sizes and t-test results between groups in Table 4. No significant changes were found between groups with effect sizes ranging from small (Right DTI-ALPS index between Cognitively normal vs MCI groups) to medium (Right DTI-ALPS index between Cognitively normal vs AD groups).

Table 5 displays partial correlations between DTI-ALPS indices and two measures of cognitive score (MMSE or ADASCog11) adjusted for age, sex and

APoE ε4 status. Significant correlations were found only in the right hemisphere with the ADASCog11 ($p < 0.009$) and MMSE ($p < 0.023$).

In Table 6, significant differences in right DTI-ALPS indices were found between cognitively normal and AD groups ($p < 0.026$) and MCI groups ($p < 0.025$) in a univariate corrected for age, sex and APoE ε4. No such differences were found with the left DTI-ALPS index. Multiple-comparison corrected values are given based on the estimated marginal means for DTI-ALPS in the model. There were also no significant changes in DTI-ALPS between MCI vs AD groups.

In Table 7, a univariate General Linear Model (GLM) corrected for age, sex and APoE ε4 is given for the Apparent Diffusion Coefficient (ADC) which is a measure of the mean diffusion in each voxel. In the projection fibres, the ADC is significant between cognitively normal and AD groups ($p < 0.028$), but falls just outside significance when multiple comparisons on the marginal means are calculated ($p < 0.057$). There were no significant results between MCI and cognitively normal groups ($p < 0.254$). There were also no significant differences found in the association fibres between any of the cognitive groups.

In Figure 3 the estimated marginal means (mean response) is shown for the right DTI-ALPS index using the GLM in Table 6 across all cognitive groups, at the mean value of the covariate (age = 72.2), adjusted for sex and APoE ε4.

Discussion

Recently, there has been considerable and growing interest in the nature of the fluid circulation in the glymphatic system, especially in the interstitial space, and driving mechanisms for this circulation. Transport in the perivascular space is believed to be advective (i.e. bulk flow) and caused by cardiac pulsatility,[1,32-34] in the parenchyma. However, some studies[35-37] have questioned the role of advection and contended that diffusion plays the most important role in the transport of neurofluids.[38-44] One recent study[45,46] used mathematic modelling to suggest both diffusion as well as advection are involved in fluid transport in the parenchyma. However, a review of such studies[47] concluded that there is a consensus that suggests diffusion is most likely the primary agent that drives fluid transport in the interstitial space.

Diffusion-weighted imaging is particularly suited to measuring CSF dynamics when compared to tracer studies because of the relatively short scanning time

involved, its non-invasive nature and its inherent sensitivity to microscopic motion. By measuring the DTI-ALPS index, this study elucidated the diffusion characteristics along the perivascular spaces of 36 participants either at risk of developing AD, living with AD, or cognitively normal controls. By overlaying SWI on T2-axial scans to exaggerate the presence of medullary arteries/veins and perivascular spaces, it was possible to draw 3mm ROIs. These ROIs were placed along the line of the medullary arteries and veins which occupy the perivascular space and which run orthogonal to white matter projection and association fibres. It was hypothesized that changes in diffusivity in these fibres may reflect changes in diffusion along the perivascular space and can be assessed with the DTI-ALPS index.[13,48]

Some other studies have made use of the DTI-ALPS index. A recent study[16] measured DTI-ALPS along the perivascular space in 25 people with Parkinson's Disease (PD), 25 people with PD with mild cognitive impairment (PD-MCI), 25 people with PDD (PD with Dementia), and 47 normal controls (ND). They found that PD-MCI ($p < 0.012$) and PDD ($p < 0.001$) participants experienced a significantly lower ALPS index than the normal controls, but no significant differences were found between the PD subgroups examined. In addition, significant correlations with MMSE were found. They concluded that the lower diffusivity values along the perivascular space were suggestive of

deterioration of the glymphatic system. Yokota et al.[15] studied the ALPS index in 24 Idiopathic Normal Pressure Hydrocephalus (iNPH) patients (12 diagnosed as pseudo-iNPH). Significant differences in ALPS index were found between the iNPH patients and controls ($p < 0.001$), pseudo-iNPH and controls ($p=0.003$), and pseudo-iNPH and iNPH ($p < 0.001$). They also performed a ROC curve analysis, and found the ALPS parameter was superior in distinguishing disease groups, compared to Evans index and callosal angle.

We were unable to find any significant differences in DTI-ALPS between cognitive groups using the groups means in an independent-samples t-test (see Table 4). However, significant partial correlations of right DTI-ALPS were shown with the cognitive test scores MMSE and ADASCog11 ($p = 0.024$ for MMSE, and $p = 0.019$ for ADASCog11. In addition, significant differences in right DTI-ALPS between normal versus MCI groups and normal versus AD groups were found in a univariate GLM correcting for age, sex and APoE ε4. No significant correlations were similarly found in the left-hemisphere which we are currently unable to explain, despite the fact the ROI placement procedures were identical.

Currently, there is a lack of literature using DTI in dementia studies for the purposes of measuring glymphatic phenomena. One recent study[49,50] used multi-shell diffusion imaging to evaluate the impact of perivascular space fluid (PVS)

on DTI values, and found that the PVS fluid can bias such results, casting a doubt on whether white matter degeneration due to ageing was entirely responsible.

The original study[13] however serves as the basis for this study. Both that study and this one used similar diffusion protocols and with the same number of diffusion gradient directions in calculating DTI-ALPS. However, our slice thickness was slighter higher (3mm) compared to 2.5mm in the earlier study. Our results though differ from it in some important respects which are as follows:

Firstly, we investigated ROIs in both hemispheres (compared to only the left hemisphere in the earlier work[13] but as a result had to reduce our regions of interest from 5mm to 3mm radius to ensure they remained entirely within the projection and association tracts in both hemispheres. We found no significant correlation between DTI-ALPS index and MMSE in the left hemisphere compared to the earlier study.[13] Results were statistically significant in the right hemisphere and only when adjusted for age, sex, and APoE ε4 which we believe very likely present a confounding influence unless the groups are a priori well-matched in these variables. Secondly, we also looked at differences between cognitive groups in a GLM model, and found significant changes in DTI-ALPS index between controls vs AD, and controls vs MCI. This may indicate reduced

glymphatic activity via impaired water diffusivity along the perivascular space in MCI and AD compared to controls, although other unknown factors cannot be discounted that may also inhibit free diffusion and restrict the flow of neurofluids in these compartments. This suggests, with further validation on larger datasets needed, that this parameter may serve as a useful imaging biomarker in identifying people with or at risk of dementia.

In this pilot study, limitations included small sample size, some variability in region of interest placement that still satisfied the same location criteria, and the retrospective nature of the study. Furthermore, our SWI images were of a higher slice thickness (4mm) than is typical. This higher slice thickness whilst improving the SNR of the SWI images, also exacerbates partial voluming affects as well as potential registration artefacts. In addition, white matter (WM) hyperintense lesions which were more prevalent amongst the AD participants can influence diffusion measures in normal appearing WM but were not adjusted for here. Aβ- Amyloid status was unfortunately not available for the AD patients, and only incomplete information for the healthy controls (80% Aβ negative) and MCI participants (also 80% Aβ negative).

As with any DTI study, high quality data, pre-processing, and accurate registrations were found to be critical in providing an accurate measurement of the DTI-ALPS index.

Registrations of both SWI and DTI pre-processed results to T2-space were performed with custom registrations scripts using ANTS and AFNI. Any errors produced in these processes, especially the standard difficulties in registration of highly atrophied AD images, may noticeably affect the final DTI-ALPS results. However, all elastic intra-subject registrations were visually assessed by interactive image blending and appeared to be of high quality for this study, with affine registrations being the major component.

In conclusion, advanced imaging of the glymphatic system may provide significant benefits to our understanding of the pathophysiology of neurological disease. Using a standard diffusion model, we found the DTI-ALPS index was able to differentiate between normal controls, MCI and AD groups. Significant correlations were also found between the DTI-ALPS index and two cognitive scores (MMSE and ADASCog11) of 36 participants either with dementia or at risk of the disease. Further imaging studies are needed to assist in improved visualization of the perivascular space in order to help validate the usefulness of

the DTI-ALPS parameter and whether it may be a biomarker of neurofluid dynamics in the glymphatic system.

References:

[1] Iliff JJ, Wang M, Liao Y, et al. A paravascular pathway facilitates CSF flow through the brain parenchyma and the clearance of interstitial solutes, including amyloid beta. Sci Transl Med 2012;4:147ra11.

[2] Jessen NA, Munk AS, Lundgaard I, Nedergaard M. The glymphatic system: A beginner's guide. Neurochem Res 2015;40:2583-99.

[3] Kress BT, Iliff JJ, Xia M, et al. Impairment of paravascular clearance pathways in the aging brain. Ann Neurol 2014;76:845-61.

[4] Agarwal N, Contarino C, Toro EF.. Neurofluids: A holistic approach to their physiology, interactive dynamics and clinical implications for neurological diseases. Veins Lymphatics 2019;8:49

[5] Mawuenyega KG, Sigurdson W, Ovod V, et al. Decreased clearance of CNS beta-amyloid in Alzheimer's disease. Science 2010;330:1774.

[6] Iliff JJ, Lee H, Yu M, et al. Brain-wide pathway for waste clearance captured by contrast-enhanced MRI. J Clin Invest 2013;123:1299-309.

[7] Siebner HR, Grafin von Einsiedel H, Conrad B. Magnetic resonance ventriculography with gadolinium DTPA: report of two cases. Neuroradiology 1997;39:418-22.

[8] Yang L, Kress BT, Weber HJ, et al. Evaluating glymphatic pathway function utilizing clinically relevant intrathecal infusion of CSF tracer. J Transl Med 2013;11:107.

[9] Eide PK, Ringstad G. MRI with intrathecal MRI gadolinium contrast medium administration: a possible method to assess glymphatic function in human brain. Acta Radiol Open 2015;4:2058460115609635.

[10] Huffman J, Phillips S, Taylor GT, Paul R.. The emerging field of perivascular flow dynamics: biological relevance and clinical applications. Technol Innov 2016;18:63-74.

[11] Kiviniemi V, Wang X, Korhonen V, et al. Ultra-fast magnetic resonance encephalography of physiological brain activity - glymphatic pulsation mechanisms? J Cereb Blood Flow Metab 2016;36:1033-45.

[12] Rivera-Rivera LA, Turski P, Johnson KM, et al. 4D flow MRI for intracranial hemodynamics assessment in Alzheimer's disease. J Cereb Blood Flow Metab 2016;36:1718-30.

[13] Taoka T, Masutani Y, Kawai H, et al. Evaluation of glymphatic system activity with the diffusion MR technique: diffusion tensor image analysis along the perivascular space (DTI-ALPS) in Alzheimer's disease cases. Jpn J Radiol 2017;35:172-8.

[14] Folstein MF, Folstein SE, McHugh PR. "Mini-mental state". A practical method for grading the cognitive state of patients for the clinician. J Psychiatr Res 1975;12:189-98.

[15] Yokota H, Vijayasarathi A, Cekic M, et al.. Diagnostic performance of glymphatic system evaluation using diffusion tensor imaging in idiopathic normal pressure hydrocephalus and mimickers. Curr Gerontol Geriatr Res 2019;2019:5675014.

[16] Chin CP, Che LW, Toshiaki T, Hsien CK, Hsien LC. Impaired glymphatic system activity in Parkinson's disease: A DTI along the perivascular space study. Presented on September 25, 2019 at OHBM 2019, Rome.

[17] Rosen WG, Mohs RC, Davis KL. A new rating scale for Alzheimer's disease. Am J Psychiatry 1984;141:1356-64.

[18] Ellis KA, Bush AI, Darby D, et al. The Australian Imaging, Biomarkers and Lifestyle (AIBL) study of aging: methodology and baseline characteristics of 1112 individuals recruited for a longitudinal study of Alzheimer's disease. Int Psychogeriatr 2009;21:672-87.

[19] Cyarto EV, Lautenschlager NT, Desmond PM, et al. Protocol for a randomized controlled trial evaluating the effect of physical activity on delaying the progression of white matter changes on MRI in older adults with memory complaints and mild cognitive impairment: the AIBL active trial. BMC Psychiatry 2012;12:167.

[20] Malpas CB, Vivash L, Genc S, et al. A phase IIa randomized control trial of VEL015 (sodium selenate) in mild-moderate Alzheimer's disease. J Alzheimers Dis 2016;54:223-32.

[21] Cardoso BR, Roberts BR, Malpas CB, et al. Supranutritional sodium selenate supplementation delivers selenium to the central nervous system: Results from a randomized controlled pilot trial in Alzheimer's disease. Neurotherapeutics 2019;16:192-202.

[22] Pierpaoli C, Walker L, Irfanoglu MO, et al. TORTOISE: an integrated software package for processing of diffusion MRI data. Presented at the 18th annual meeting of the ISMRM. May 2010; Stockholm, Sweden.

[23] Irfanoglu MO, Nayak A, Jenkins J, et al. TORTOISE v3:Improvements and new features of the NIH diffusion MRI processing pipeline. Presented at the 25th annual meeting. of the ISMRM. April 2017; Honolulu, HI.

[24] Cox RW. AFNI: software for analysis and visualization of functional magnetic resonance neuroimages. Comput Biomed Res 1996;29:162-73.

[25] Avants BB, Epstein CL, Grossman M, Gee JC. Symmetric diffeomorphic image registration with cross-correlation: evaluating automated labeling of elderly and neurodegenerative brain. Med Image Anal 2008;12:26-41.

[26] McCarthy P. FSLeyes. https://zenodo.org/record/3937147, Accessed on July 9th, 2020.

[27] Thurfjell L, Lilja J, Lundqvist R, et al. Automated quantification of 18F-flutemetamol PET activity for categorizing scans as negative or positive for brain amyloid: concordance with visual image reads. J Nucl Med 2014;55:1623-8.

[28] Crook TH, 3rd, Feher EP, Larrabee GJ. Assessment of memory complaint in age-associated memory impairment: the MAC-Q. Int Psychogeriatr 1992;4:165-76.

[29] Welsh KA, Butters N, Mohs RC, et al. The Consortium to Establish a Registry for Alzheimer's Disease (CERAD). Part V. A normative study of the neuropsychological battery. Neurology 1994;44:609-14.

[30] McKhann G, Drachman D, Folstein M, Katzman R, Price D, Stadlan EM. Clinical diagnosis of Alzheimer's disease: report of the NINCDS-ADRDA Work Group under the auspices of Department of Health and Human Services Task Force on Alzheimer's Disease. Neurology 1984;34:939-44.

[31] IBM Corp. IBM SPSS Statistics for Windows [Internet]. Armonk, NY: IBM Corp; 2017.

[32] Iliff JJ, Wang M, Zeppenfeld DM, et al. Cerebral arterial pulsation drives paravascular CSF-interstitial fluid exchange in the murine brain. J Neurosci 2013;33:18190-9.

[33] Rennels ML, Gregory TF, Blaumanis OR, Fujimoto K, Grady PA. Evidence for a 'paravascular' fluid circulation in the mammalian central nervous system, provided by the rapid distribution of tracer protein throughout the brain from the subarachnoid space. Brain Res 1985;326:47-63.

[34] Mestre H, Tithof J, Du T, et al. Flow of cerebrospinal fluid is driven by arterial pulsations and is reduced in hypertension. Nat Commun 2018;9:4878.

[35] Cserr HF. Role of secretion and bulk flow of brain interstitial fluid in brain volume regulation. Ann N Y Acad Sci 1988;529:9-20.

[36] Cserr HF, Depasquale M, Patlak CS, Pullen RG. Convection of cerebral interstitial fluid and its role in brain volume regulation. Ann N Y Acad Sci 1986;481:123-34.

[37] Weed LH. Studies on cerebro-spinal fluid. No. III : The pathways of escape from the subarachnoid Spaces with particular reference to the arachnoid villi. J Med Res 1914;31:51-91.

[38] Smith AJ, Verkman AS. The "glymphatic" mechanism for solute clearance in Alzheimer's disease: game changer or unproven speculation? FASEB J 2018;32:543-51.

[39] Smith AJ, Yao X, Dix JA, Jin BJ, Verkman AS. Test of the 'glymphatic' hypothesis demonstrates diffusive and aquaporin-4-independent solute transport in rodent brain parenchyma. Elife 2017;6.e27679.

[40] Jin BJ, Smith AJ, Verkman AS. Spatial model of convective solute transport in brain extracellular space does not support a "glymphatic" mechanism. J Gen Physiol 2016;148:489-501.

[41] Abbott NJ, Pizzo ME, Preston JE, Janigro D, Thorne RG. The role of brain barriers in fluid movement in the CNS: is there a 'glymphatic' system? Acta Neuropathol 2018;135:387-407.

[42] Smith AJ, Verkman AS. CrossTalk opposing view: Going against the flow: interstitial solute transport in brain is diffusive and aquaporin-4 independent. J Physiol 2019;597:4421-4.

[43] Smith AJ, Verkman AS. Rebuttal from Alex J. Smith and Alan S. Verkman. J Physiol. 2019;597:4427-8.

[44] Simon M, Iliff J. Rebuttal from Matthew Simon and Jeffrey Iliff. J Physiol 2019;597:4425-6.

[45] Koundal S, Elkin R, Nadeem S, et al. Publisher Correction: Optimal mass transport with lagrangian workflow reveals advective and diffusion driven solute transport in the glymphatic system. Sci Rep 2020;10:3934.

[46] Koundal S, Elkin R, Nadeem S, et al. Optimal mass transport with lagrangian workflow reveals advective and diffusion driven solute transport in the glymphatic system. Sci Rep 2020;10:1990.

[47] Martinac AD, Bilston LE. Computational modelling of fluid and solute transport in the brain. Biomech Model Mechanobiol 2020;19:781-800.

[48] Taoka T, Naganawa S. Glymphatic imaging using MRI. J Magn Reson Imaging 2020;51:11-24.

[49] Sepehrband F, Barisano G, Sheikh-Bahaei N, et al. Image processing approaches to enhance perivascular space visibility and quantification using MRI. Sci Rep 2019;9:12351.

[50] Sepehrband F, Cabeen RP, Choupan J, Barisano G, Law M, Toga AW. Alzheimer's Disease Neuroimaging I. Perivascular space fluid contributes to diffusion tensor imaging changes in white matter. Neuroimage 2019;197:243-54.

Table 1. Demographics, Sex (0 male, 1 female), MMSE, ADAS-cog11, Cognition Status (0 for cognitively normal, 1 for MCI, and 2 for AD), and APoE ε4 (1 for ε4 positive and 0 for ε4 negative).

Participant	Age (years)	Sex	MMSE	ADAS-cog11	APoE ε4	Cognition Status
1	76	1	28	6.00	.00	0
2	75	0	29	5.00	.00	0
3	74	0	30	10.00	.00	0
4	73	1	30	11.00	1.00	0
5	74	0	29	3.00	1.00	0
6	76	1	30	4.00	.00	0
7	71	1	29	3.00	.00	0
8	84	1	28	12.00	.00	0
9	65	0	29	8.00	1.00	0
10	70	0	28	10.00	.00	0
11	77	0	29	15.00	.00	1
12	88	1	29	12.00	1.00	1
13	69	1	30	7.00	.00	1
14	72	0	27	13.00	.00	1
15	67	0	29	8.00	1.00	1
16	73	1	29	7.00	1.00	1

17	89	1	28	14.00	.00	1
18	79	1	28	8.00	.00	1
19	67	1	30	5.00	.00	1
20	80	0	29	13.00	.00	1
21	68	0	16	37.00	1.00	2
22	66	0	22	24.33	.00	2
23	63	1	20	17.00	.00	2
24	59	0	15	36.66	1.00	2
25	62	0	18	14.33	1.00	2
26	65	0	14	31.67	1.00	2
27	73	0	28	19.00	1.00	2
28	62	1	17	18.33	1.00	2
29	81	0	19	19.33	.00	2
30	63	1	17	26.00	1.00	2
31	69	0	25	19.66	1.00	2
32	75	1	15	27.66	1.00	2
33	78	1	13	34.33	1.00	2
34	67	0	16	33.00	.00	2
35	82	0	28	9.67	1.00	2
36	73	0	16	14.33	.00	2

Table 2. Mean and Standard Deviation (or range) for demographics organized by cognitive group (Normal, MCI and AD) and comparison with source trial data.

	Cognitively Normal (Aibl Active)			MCI (Aibl Active)			AD (VEL015)		
	Entire Cohort (N=77)	Study Cohort (N=10)	p-value	Entire Cohort (N=31)	Study Cohort (N=10)	p-value	Entire Cohort (N=40)	Study Cohort (N=16)	p--value
Age (Years)	72.97 (5.94)	73.80 (4.89)	0.70	73.45 (5.75)	76.10 (7.99)	0.30	71 (61-81)	69.13 (59-82)	0.61
Sex (Female, %)	42 (54.45%)	5 (50%)	0.79	15 (48.39%)	6 (60%)	0.52	17 (42.5%)	5 (31%)	*0.83*
APoE ε4 (ε4+, %)	19 (24.6%)	3 (30%)	0.72	10 (32.26%)	3 (30%)	0.89	27 (67.5%)	11 (69%)	0.43
MMSE	29.18 (1.04)	28.5 (0.97)	0.07	28.35 (1.68)	28.3 (1.57)	0.94	20 (2)	18.7 (4.73)	0.45
ADASCog11	6.06 (3.11)	6.30 (2.98)	0.81	9.55 (4.58)	8.60 (3.03)	0.46	22.08 (5.17)	23.9 (8.69)	0.71

N=number of participants, Aibl: Australian Imaging, Biomarkers and Lifestyle

Table 3. Mean ± standard deviation values of DTI-ALPS indices between cognitive groups

Cognitive Group	Right DTI-ALPS	Left DTI-ALPS
ALL	1.5198 ± 0.1920	1.4540 ± 0.1578
Cognitively normal	1.5812 ± 0.2258	1.4830 ± 0.1671
MCI	1.5043 ± 0.2314	1.4346 ± 0.1644
AD	1.4912 ± 0.1400	1.4479 ± 0.1557

Table 4. Effect size (Cohen's d) and t-test results for the left and right DTI-ALPS parameter between cognitive groups.

	Right DTI-ALPS	Left DTI-ALPS
Cognitively normal vs MCI	0.34 (p=0.46)	0.29 (p=0.52)
Cognitively normal vs AD	0.48 (p=0.22)	0.22 (p=0.59)
MCI vs AD	0.07 (p=0.86)	0.08 (p=0.84)

Effects sizes are medium for normal vs MCI and normal vs AD groups.

Table 5. Partial Correlation (bootstrapping with 1000 iterations) for DTI-ALPS index and cognitive score (MMSE or ADASCog11) adjusted for age, sex, and APoE ε4.

	MMSE	ADASCog11
Right DTI-ALPS	r (31) = 0.394 p =0.023	r (31) = -0.448 p = 0.009
Left DTI-ALPS	r (31) = 0.271 p = 0.128	r (31) = -0.264 p = 0.137

Table 6. Univariate GLM for right DTI-ALPS index between cognitively normal, MCI and AD groups, adjusted for age, sex, and APoEε4.

	Contrast Estimate	Hypothesized Value	Difference (Estimate - Hypothesized)	Standard Error	Significance.	Sig.Significance (multiple comparison corrected)	95% Confidence Interval for Difference (Lower)	95% Confidence Interval for Difference (Upper)
MCI vs. Cognitively normal	-.219	0	-.219	.091	p=.025	p=.024	-.407	-.031
AD vs. Cognitively normal	-.215	0	-.215	.091	p=.026	p=.034	-.403	-.028

GLM=General Linear Model, ADC=-Apparent Diffusion Coefficient

Table 7. Univariate GLM for ADC (mean diffusion) in the right projection fibres between cognitively normal, MCI and AD groups, adjusted for age, sex, and APoEε4.

	Contrast Estimate	Hypothesized Value	Difference (Estimate - Hypothesized)	Standardtd. Error	Significance.	Significance. (multiple comparison corrected)	95% Confidence Interval for Difference (Lower)	95% Confidence Interval for Difference (Upper)
MCI vs. Cognitively normal	-41.228	0	-41.228	35.234	p=.254	p=.454	-114.116	31.660
AD vs. Cognitively normal	-84.765	0	-84.765	36.256	p=.028	p=.057	-159.766	-9.764

GLM=General Linear Model, ADC=-Apparent Diffusion Coefficient

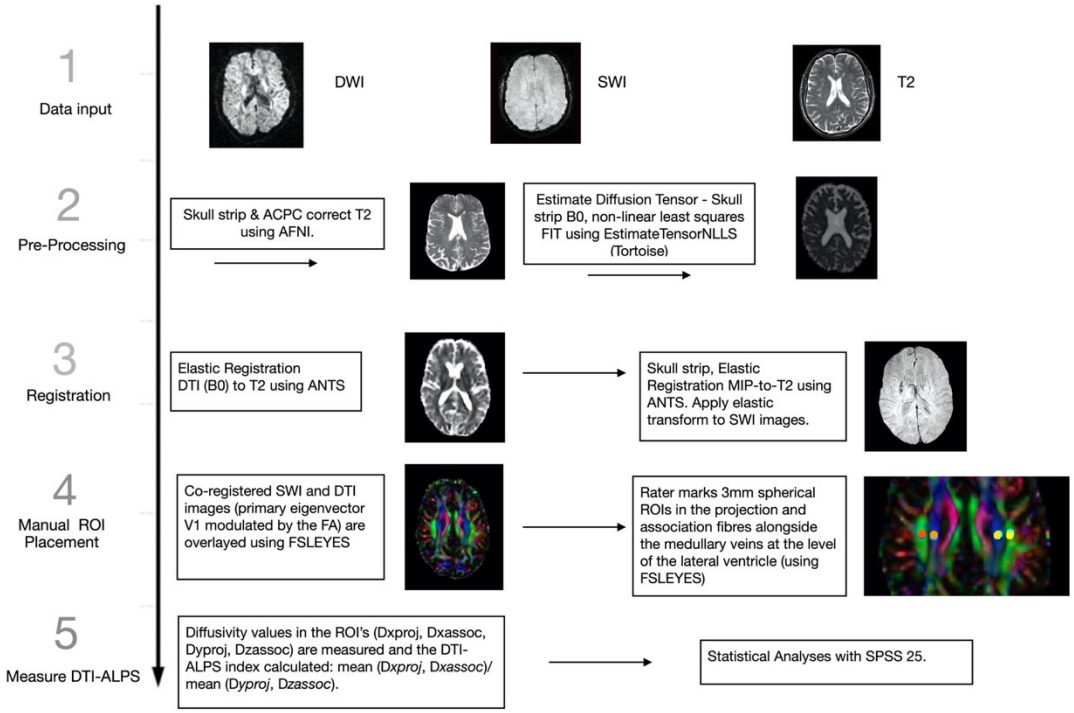

Figure 1 – Pictorial description of the major elements of the image processing pipeline. With Diffusion Weighted Images (DWI), Susceptibility Weighted Images (SWI) and T2 data in (1), the T2 data is skull-stripped and AC-PC corrected using default AFNI scripts in (2). The diffusion data is skull-stripped, and a non-linear least squares method employed to fit the diffusion tensor using AFNI's DTI tools. In (3), the B0 image is elastically registered to the T2-scans using ANTS, and the transformation applied to the full tensor. In this way, the primary eigenvector and standard DTI metrics are now in T2-space. The MIP images are skull-stripped using AFNI, and registered (with ANTS) to the same T2-data. The affine and warp transformations from this are applied to the SWI data to move it into T2-space. In (4), the primary eigenvector (scaled by the FA) is overlaid on the SWI data using FSL's visualisation tool, FSLEYES. A rater then marked 3mm spherical Regions of Interest (ROI's) in the projection and association fibres at the level of the lateral ventricles. In (5), the diffusivity values in these regions of interest were used to calculate the DTI-ALPS index, which served as input to all subsequent statistical tests in SPSS 25.

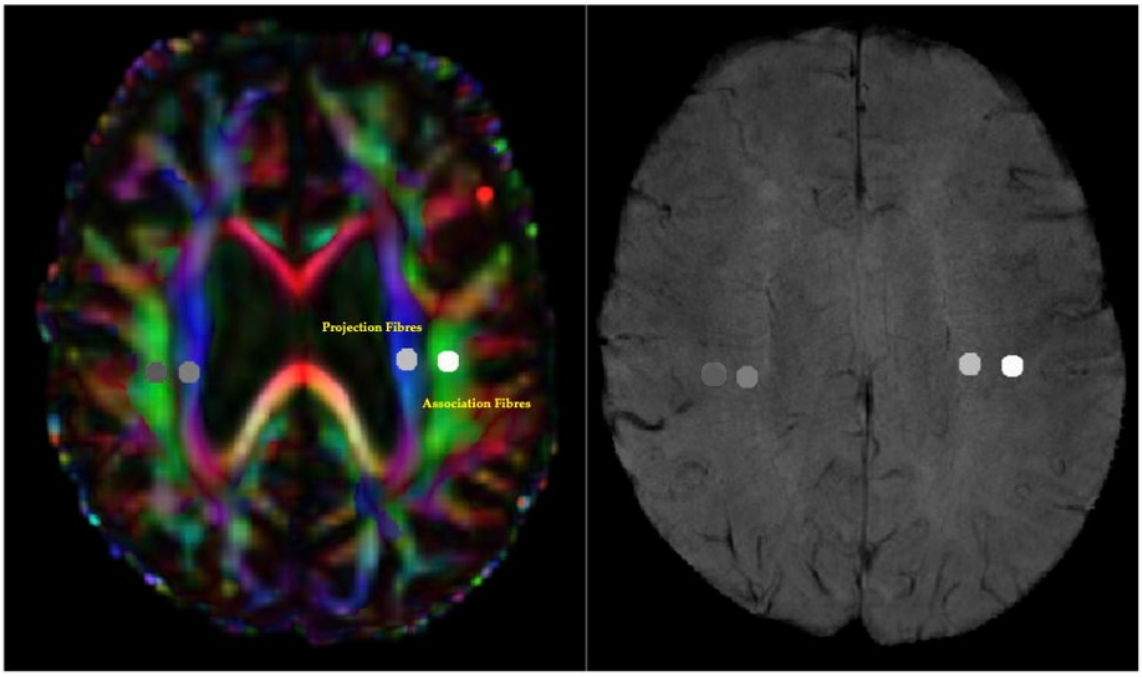

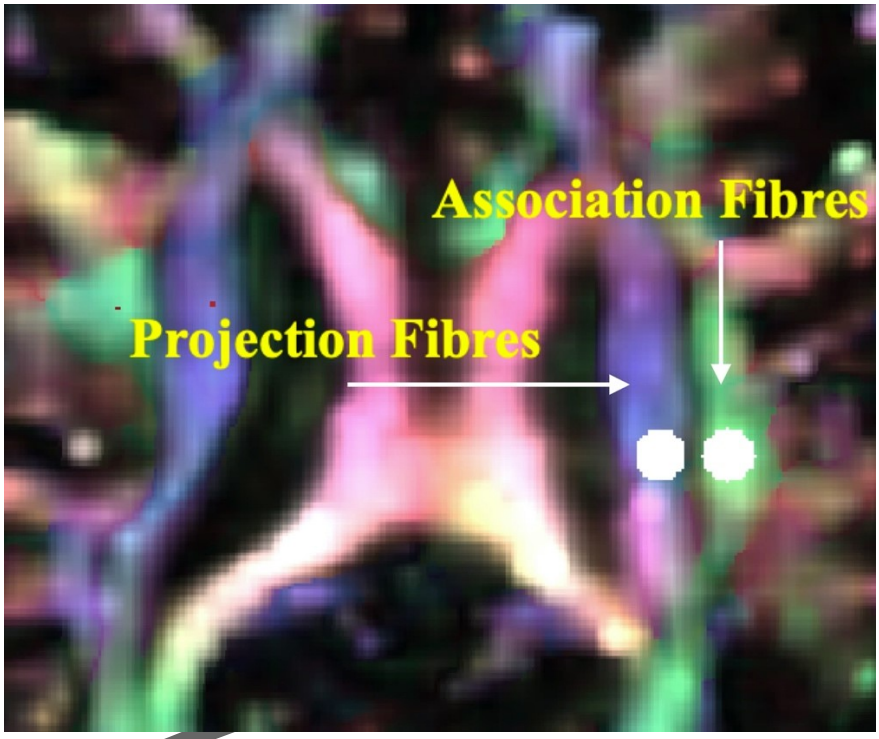

Figure 2a and 2b – In Fig 2a, on the left, the primary eigenvector (V1) modulated by the Fractional Anisotropy and on the right, the

corresponding SWI images for one patient. *Regions of Interest* (ROI) masks in the projection fibres (blue (z axis)) and association fibres (green (y axis)) are indicated. Fig 2b below shows a zoomed image of the fibres with 3mm sample ROIs shown in grey in the left hemisphere. The arrows point to both Projection and Association Fibre regions.

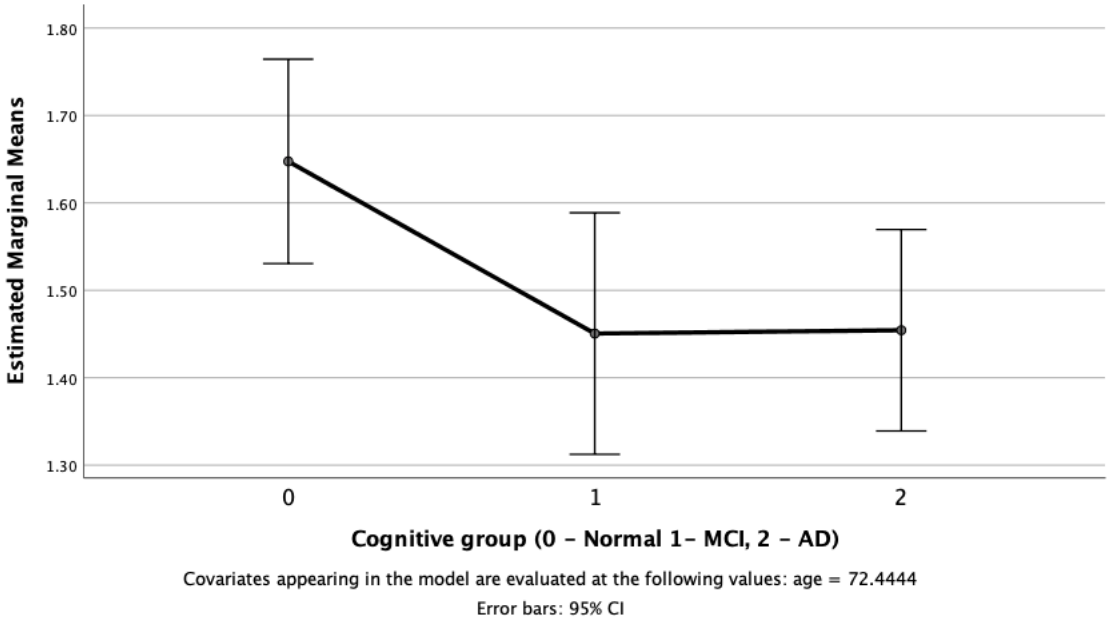

Figure 3. Estimated Marginal Means from the General Linear Model for right DTI-ALPS index between cognitively normal, MCI and AD groups, adjusted for age, gender, and APoEe4.